Bed topography of Princess Elizabeth Land in East Antarctica

Xiangbin Cui[1], Hafeez Jeofry[2,3], Jamin S Greenbaum[4], Jingxue Guo[1], Lin Li[1], Laura E Lindzey[5], Feras A Habbal[6], Wei Wei[4], Duncan A Young[4], Neil Ross[7], Mathieu Morlighem[8], Lenneke M. Jong[9,10], Jason L Roberts[9,10], Donald D Blankenship[4], Sun Bo[1] and Martin J. Siegert[11]

[1] Polar Research Institute of China, Jinqiao Road, Shanghai, China
[2] Faculty of Science and Marine Environment, Universiti Malaysia Terengganu, Kuala Terengganu, Terengganu, Malaysia
[3] Institute of Oceanography and Environment, Universiti Malaysia Terengganu, Kuala Terengganu, Terengganu, Malaysia
[4] Institute for Geophysics, Jackson School of Geosciences, The University of Texas at Austin, Austin, Texas, USA
[5] Department of Ocean Engineering, Applied Physics Laboratory, University of Washington, USA
[6] Oden Institute for Computational Engineering and Sciences, University of Texas at Austin
[7] School of Geography, Politics and Sociology, Newcastle University, Newcastle upon Tyne, UK
[8] Department of Earth System Science, University of California Irvine, Irvine, California, USA
[9] Australian Antarctic Division, Kingston, Tasmania, Australia
[10] Institute for Marine and Antarctic Studies, University of Tasmania, Hobart, Tasmania
[11] Grantham Institute and Department of Earth Science and Engineering, Imperial College London, South Kensington, London, UK

Abstract

We present a topographic digital elevation model (DEM) for Princess Elizabeth Land (PEL), East Antarctica. The DEM covers an area of ~900,000 km^2 and was established from RES data collected in four campaigns since 2015. Previously, the region (along with Recovery basin elsewhere in East Antarctica) was characterised by an inversion using low resolution satellite gravity data across a large (>200 km wide) data-free zone to generate the Bedmap2 topographic product. We use the mass conservation (MC) method to produce an ice thickness grid across faster-flowing (>30 m yr^{-1}) regions of the ice sheet and streamline diffusion in slower-flowing areas. The resulting ice thickness model is integrated with an ice surface model to build the bed DEM. Together with BedMachine Antarctica, and Bedmap2, this new bed DEM completes the first order measurement of subglacial continental Antarctica – an international mission that began around 70 years ago. The ice thickness and bed elevation DEMs of PEL (resolved horizontally at 500 m relative to ice surface elevations obtained from the Reference Elevation Model of Antarctica) are accessible from http://doi.org/10.5281/zenodo.4023343 (Cui et al., 2020).

1. Introduction

Radio-echo sounding (RES) is commonly used to measure ice thickness, and to understand subglacial topography and basal ice-sheet conditions (Dowdeswell and Evans, 2004; Bingham and Siegert, 2007). A series of airborne geophysical explorations were conducted across East Antarctica in the 1970s (Robin et al., 1977; Dean et al., 2008; Turchetti et al., 2008; Naylor et al., 2008), which led to the first compilation 'folio' maps of subglacial bed topography, ice-sheet surface elevation and ice thickness of Antarctica (Drewry and Meldrum, 1978; Drewry et al., 1980; Jankowski and Drewry, 1981; Drewry, 1983). Since then, multiple efforts have been made to collect and compile RES data in order to expand the RES database across the continent (Lythe et al., 2001; Fretwell et al. 2013). The first geophysical exploration of the coast of Princess Elizabeth Land (PEL) was conducted between 1971–2016, providing basic ice thickness, bed topography and magnetic field data (Popov and Kiselev, 2018; Popov, 2020). To date, virtually no RES data have been acquired upstream of ~300 km from the grounding line of PEL. Hence, this region has been described as one of the so-called 'poles of ignorance' (Fretwell et al., 2013) and its representation in recent bed DEMs (Bedmap2 and BedMachine Antarctica) is as a zone of flat topography, reflecting the absence of RES data (Morlighem et al., 2020). Indeed, other data gaps (Recovery system, Diez et al., 2019; and South Pole, Jordan et al, 2018) have been filled recently, leaving PEL as the last remaining significant region in Antarctica to be surveyed systematically.

In the absence of bed data, glaciologists have had to rely on satellite imagery, inversion from poor resolution satellite gravity observations, and ice-flow modelling to infer the subglacial landscape and its interaction with the ice above (Fretwell et al., 2013; Jamieson et al., 2016). For example, combination of three satellite-derived mosaics, and some initial exploratory RES data (Blankenship et al., 2017), have been used to hypothesise the subglacial features of PEL, revealing the presence of a potentially large (>100 km long) subglacial lake (white box; Figure 1a and 1b) and an expected canyon morphology across the PEL sector. Previously, a study by Dongchen et al. (2004) adopted the interferometric synthetic-aperture radar (InSAR) satellite technology to generate an 'experimental' subglacial bed elevation model across the ice sheet margin. While the result contains a level of 'detail', it has an obvious limitation in that the bed elevation was based solely on the satellite data and without direct measurement of the subglacial landscape. Another study used an inversion technique to generate a 'synthetic' glacier thickness of the PEL region from satellite gravity data, as part of the Bedmap2 compilation (Fretwell et al., 2013). A qualitative inspection of the Bedmap2 bed elevation product reveals the bed of PEL to be anomalously flat –a consequence of its use of satellite gravity data in a low-resolution inversion for bed elevation across a data-free region. Hence, the bed topography in PEL is the poorest-defined of any region in Antarctica – and indeed of any land surface on Earth.

Here, we present the first detailed ice thickness DEM for PEL, based on new RES measurements collected since 2015, which we refer to as the 'ICECAP2' DEM. We briefly discuss the differences between the ICECAP2 DEM and its representation in both Bedmap2 and BedMachine Antarctica. The ICECAP2 bed DEM is relative to ice surface elevations from the Reference Elevation Model of Antarctica (Howat, et al., 2019). The ice thickness DEM can be easily integrated with updated surface DEMs (i.e. Helm et al., 2014) and, in particular, the upcoming Bedmap3 product.

2. Study Area

The PEL sector of East Antarctica is bounded on the west by the Amery Ice Shelf, and on the east by Wilhelm II Land (Figure 1a). The region covered by the ICECAP2 DEM we present here extends ~1,300 km from East to West and ~800 km from North to South. In comparison with Bedmap2, the ICECAP2 DEM benefits from recently acquired airborne geophysical data collected by the ICECAP2 programme over four austral summer seasons from 2015 to 2019 (Figure 1c). We use the Differential Interferometry Synthetic Aperture Radar (DInSAR) grounding line (Rignot et al., 2011) to delimit the ice-shelf facing margin of the ice sheet.

3. Data and Methods

During the first field season (2015/16), a survey acquiring exploratory 'fan-shaped' radial profiles, to maximize range and data return on each flight, was completed across the broadly unknown region of PEL. These flight lines extend from the coastal Progress Station to the interior ice-sheet divide at Ridge B (Figure 1a). In the second and third seasons (2016/17 and 2017/18), a survey 'grid' was completed, targeting enhanced resolution over a proposed subglacial lake and a series of basal canyons (see Jamieson et al., 2016). In the fourth season (2018/19), a few additional transects were completed to fill the largest data gaps within aircraft range.

Field data acquisition was achieved using the "Snow Eagle 601" aerogeophysical platform; a BT-67 airplane operated by the Polar Research Institute of China for the Chinese National Antarctic Research Expedition (CHINARE) program (Figure 2a and b). The suite of instruments configured on the airplane include a phase coherent RES system, functionally similar to the High Capability Airborne Radar Sounder developed by the University of Texas Institute for Geophysics (UTIG) (i.e. Young et al., 2011; Greenbaum et al., 2015). HiCARS is a phase coherent RES system, operating at a central frequency of 60 MHz and a peak power of 8 kW, making it capable of penetrating deep (>3 km) ice in Antarctica. After applying coherent integration and pulse compression at a bandwidth of 15 MHz, which gave an along-track spatial sampling rate and a vertical resolution of ~20 m and ~5.6 m, respectively. Further details on the parameters and introduction of the RES system can be found in Cui et al. (2018). A JAVAD GPS receiver and its four antennas are mounted at the aircraft centre of gravity (CG), tail and both wings. GPS data from antenna at the aircraft CG were used for RES data interpretation.

4. Data Processing

Ice thickness measurements were derived from two RES data products from which the ice-bed interface was traced and digitized: (a) 2D focused SAR processed data applied to RES data from the first two seasons; and (b) unfocused 'field' RES data from the third and fourth seasons. Raw RES data were first separated to differentiate PST (Project/Set/Transect) during the field data processing. Pulse compression, filtering, 10-traces coherent stacking and 5-traces incoherent stacking were then applied to generate a field RES data product. The field RES data can be used for quality control and are also good enough for initial ice-bed interface measurements, from which a first-order ice thicknesses and bed elevation DEM was calculated. To achieve better-quality RES images, two-dimensional focused SAR processing was applied to data from the first two seasons (Peters et al., 2007). The ice-bed interface was picked in a semi-automatic manner using a picking program used previously by the ICECAP program on data from the Aurora and Wilkes subglacial basins (Blankenship et al., 2016; Blankenship et al., 2017). Ice thicknesses were calculated from multiplying two-way travel time by the velocity of electromagnetic waves in ice (i.e. 0.168 m ns^{-1}) (Cui et al., 2018). Firn corrections were not applied, and thus may be subject to a small systematic error. The precise point positioning (PPP) method was used in the GPS processing to improve positioning accuracy since the flight distance is too far from the GPS base station for post airborne GPS data processing. Processed GPS data were interpolated and fitted to the radar traces according to time stamps generated by the integrated airborne system. Aircraft to ice-surface range was calculated by multiplying the two-way travel time of the radar reflections of the ice surface by its velocity in air (0.3 m ns^{-1}). Figure 2c shows examples of the RES images from the data collected in 2017/18.

To derive the ice thickness map (Figure 4a), we employed a variety of techniques depending on the ice speed following the approach described in Morlighem et al. (2020). In fast flowing regions (i.e. velocity >30 m yr^{-1}), we relied on mass conservation (MC; Figure 3), constrained by the ICECAP2 RES data and additional RES data that were available as part of BedMachine Antarctica (Morlighem et al., 2020). In the slower moving regions inland, we relied on a streamline diffusion interpolation to fill between data points (Figure 3).

For the purpose of comparing the ICECAP2 DEM (Figure 4b) with Bedmap2 (Figure 4c) and BedMachine Antarctica (Figure 4d), the 500 m ice-surface elevation DEM from The Reference Elevation Model of Antarctica (Howat et al., 2019) was used. Prior to the subtraction process, the Bedmap2 and BedMachine ice thickness DEMs were transformed from the g104c geoid vertical reference to WGS 1984 vertical reference frame. The ice thickness for both Bedmap2 and BedMachine are in "ice equivalent" rather than an estimation of the physical ice thickness from firn correction. The Bedmap2 and BedMachine ice thickness DEMs were resampled using the "Bilinear" function in ArcGIS to a 500 m spacing and referenced to the polar stereographic projection (Snyder, 1987). The ice thickness from all three models were then subtracted from the ice surface elevation DEM (Howat et al., 2019) to produce a bed DEMs at 500 m resolution. Difference maps were then computed by subtracting the Bedmap2 (Figure 4e) and BedMachine (Figure 4f) bed DEMs from the ICECAP2 bed DEM. Crossover analyses show RMS errors of 24.2 m (2015/16), 39.2 m (2016/17), 10.4 m (2017/18), 7.5 m (2018/19) and 35.4 m (for the full dataset).

5. Results

5.1 Subglacial morphology of Princess Elizabeth Land

The ICECAP2 RES data allow us to form an appreciation of the subglacial topography of PEL (Figure 4a and b). While its hypsometry (Figure 5) reveals an area-elevation distribution that is mainly concentrated around 0 to 500 m (>15% frequency, Figure 5a) with a mean elevation of 233.44 m, the DEM reveals a newly-discovered broad, low-lying subglacial basin (>250 m below sea level; Figure 4b, black box). This is the most distinct new topographic feature uncovered by the ICECAP2 data. The data also resolve higher ground across the northwest grid of the ICECAP2 DEM (Figure 5a). A deep (i.e. ~1000m below sea level) subglacial trough can be observed near to Zhaojun Di area, coinciding with the location of fast ice flow towards the Amery Ice Shelf (Figure 1a). Mountains beneath Ridge B (Figure 1a) can be observed in enhanced resolution from the ICECAP2 data (Figure 5b) with an average elevation of ~1500 m above sea level. The bed topography closer to the grounding line (i.e. Wilhelm II Land) and at the central grid areas are characterized as having a lower bed elevation (below sea level, Figure 5b), consistent with the recent BedMachine Antarctica product (Morlighem et al., 2020). Subglacial troughs with depth less than ~500 m can also be observed in Wilhelm II Land.

5.2 Comparison with Bedmap2 and BedMachine Antarctica

The ICECAP2 DEM of PEL, the corresponding Bedmap2 and BedMachine DEMs, and maps displaying differences between the three are shown in Figure 4b-f. The ICECAP2 DEM reveals substantial changes relative to Bedmap2 and BedMachine bed products especially across the central upstream region of PEL. For example, the ICECAP2 DEM shows noticeable disagreement from Bedmap2 across the

Australian Antarctic Territory extending from the central grid of the DEM (i.e. Korotkevicha Plateau and King Leopold and Queen Astrid Coast) to the Mason Peaks at the northern grid, with mean difference of ~-230m. However, the bed elevation is higher in the ICECAP2 bed DEM compared with Bedmap2 across Wilhelm II Land with a mean difference of ~170m and near to the SPRI-60 subglacial lake with mean difference of ~230m. A significant difference can also be seen between ICECAP2 and BedMachine bed DEMs across the central grid of the DEM. The ICECAP2 DEM is shown lower in bed elevation relative to BedMachine with mean difference of ~-400m. Because the ICECAP2 bed DEM is higher in some places compared with Bedmap2 and BedMachine, and lower in others, the mean differences for the entire PEL study area are only -18m and -79m, respectively.

We also present five terrain profiles for both DEMs (Figure 6), which collectively cover most of the PEL sector (Figure 1c). The purpose is to capture as much of the subglacial morphology as possible and assess the accuracy of the DEMs in their characterization of these subglacial features. In general, and as one would expect, the ICECAP2 bed DEM shows reasonable agreement with the RES transects in all profiles compared with Bedmap2 bed DEM. Consistencies between the ICECAP2 DEM and the bed elevation from RES data picks can be seen upstream of the ICECAP2 DEM grid (i.e. Mason Peaks and Zhaojun Di) with a correlation coefficient of 0.83 (RE:3%) and 0.97 (RE:1%) for Profile A and B, respectively. This is higher relative to both the Bedmap2 and BedMachine DEMs, which are 0.74 (RE:19%) and 0.56 (RE:36%) for Profile A, and 0.89 (RE:11%) and 0.07 (RE:26%) for Profile B, respectively. A significant improvement is also noted in the ICECAP2 DEM across the American Highland in Profile C (Figure 6), with a correlation coefficient of 0.91 (RE:5%), compared with 0.59 (RE:9%) for Bedmap2 and 0.33 (RE:11%) for BedMachine. A slightly lower correlation coefficient quantified for the ICECAP2 DEM in Profile D, at 0.85 (RE:17%), but it is still higher than in Bedmap2 at 0.57 (RE:32%) and BedMachine at 0.54 (RE:48%). In Profile E (near to Wilhelm II Land), the ICECAP2 DEM correlation coefficient is slightly higher at 0.91 (RE:0.5%) than BedMachine at 0.87 (RE:0.37%), and much higher than in Bedmap2 at 0.57 (RE:40%).

6. Data availability

The ICECAP2 ice thickness and bed elevation models of the PEL sector are available in 500 m horizontal resolutions at http://doi.org/10.5281/zenodo.4023343 (Cui et al., 2020). The airborne radio-echo sounder ice thickness measurements used to generate the products, recorded here in comma-separated values (CSV) format is accessible from http://doi.org/10.5281/zenodo.4023393. The 500 m ice-sheet surface elevation DEM derived from the Reference Elevation Model of Antarctica (Howat, et al., 2019) can be obtained from https://www.pgc.umn.edu/data/rema/. If the users wish to modify the bed DEM, our model can be easily integrated with the updated surface elevation models (Bamber et al., 2009; Helm et al., 2014). Auxiliary details for the MEaSUREs InSAR ice velocity map of Antarctica can be found at https://doi:10.5067/MEASURES/CRYOSPHERE/nsidc-0484.001. The satellite images for MODIS Mosaic of Antarctica 2008-2009 and RADARSAT (25m) are obtainable from https://doi.org/10.7265/N5KP8037 and https://research.bpcrc.osu.edu/rsl/radarsat/data/, respectively. A summary of the data used in this paper and their availability is provided in the Table 1.

7. Summary

We have compiled the first airborne RES dataset for PEL; acquired by ICECAP2 and led by PRIC. From the data, using a combination of interpolation and modelling techniques, we have generated a bed DEM at a higher resolution of 500 m for ice sheet modelling. The DEM has a total area of ~899,730 km^2. Considerable variabilities between the ICECAP2 DEM and Bedmap2 and BedMachine Antarctica are observed, particularly at the central grid of the DEM where a broad subglacial basin has been identified and measured. The ICECAP2 DEM completes the first-order data coverage of subglacial Antarctica – a feat spanning around 70 years of international collaboration.

Acknowledgements

This paper is a contribution of the ICECAP2 consortium (International Collaborative Exploration of Central East Antarctica through Airborne geophysical Profiling) led by SB, JLR, DDB and MJS. The research was supported by the Chinese Polar Environmental Comprehensive Investigation and Assessment Programs (CHINARE-02-02), the National Natural Science Foundation of China (41941006) and the National Key R&D Program of China (2019YFC1509102). MJS acknowledges support from the British Council's Global Innovation Initiative between the UK, USA, China and India. We thank the volunteers at QGIS for open-source software used to draw many of the figures in this paper. DDB, JG and DY acknowledge the G. Unger Vetlesen Foundation, and US National Science Foundation grants PLR-1543452 and PLR- 1443690. JR acknowledges the Australian Antarctic Division, which provided funding and logistical support (AAS 4346 and 4511). This work was also supported by the Australian Government's Cooperative Research Centres Programme through the Antarctic Climate & Ecosystems Cooperative Research Centre and under the Australian Research Council's Special Research Initiative for Antarctic Gateway Partnership (Project ID SR140300001). This is UTIG contribution ####.

Competing Interests

The authors report no competing interests for this paper.

Author contributions

XB, JSG, JG, LL, LEL, FH, WW, LJ and JRL undertook fieldwork and data acquisition. JSG and DAY undertook data processing. MM and HJ undertook data interpolation. All authors comments and edited drafts of this paper. The paper was written by MJS and HJ.

Table 1: Data files and locations.

Products	Files	Location	DOI/URL
Bed elevation DEM	500 m bed elevation DEM	Zenodo Data Repository Cui et al. (2020)	http://doi.org/10.5281/zenodo.4023343
Ice thickness DEM	500 m ice thickness DEM	Zenodo Data Repository Cui et al. (2020)	http://doi.org/10.5281/zenodo.4023343
Airborne ice thickness data	Polar Research Institute of China ice thickness data in CSV format	Zenodo Data Repository Cui et al., (2020)	http://doi.org/10.5281/zenodo.4023393
1 km ice sheet surface DEM	ERS-1 radar and ICESat laser satellite altimetry	National Snow and Ice Data Center (NSIDC)	https://nsidc.org/data/docs/daac/nsidc0422_antarctic_1km_dem/
Ice velocity map of Central Antarctica	MEaSUREs InSAR-based ice velocity	National Snow and Ice Data Center (NSIDC)	https://doi:10.5067/MEASURES/CRYOSPHERE/nsidc-0484.001
Ice sheet surface satellite imagery	MODIS Mosaic of Antarctica (2008 – 2009) (MOA2009)	National Snow and Ice Data Center (NSIDC)	https://doi.org/10.7265/N5KP8037
	RADARSAT (25m) satellite imagery	Byrd Polar and Climate Research Center	https://research.bpcrc.osu.edu/rsl/radarsat/data/

(a)

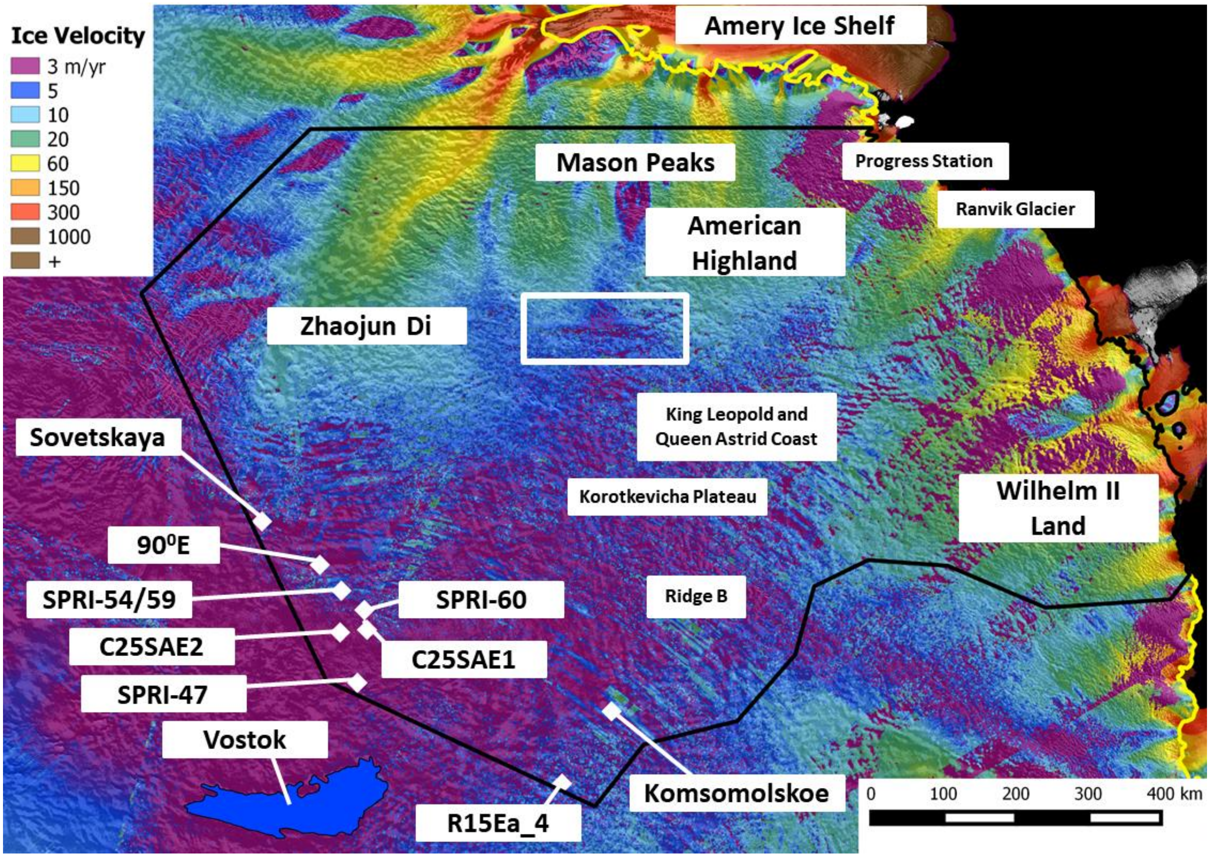
Ice Velocity
3 m/yr
5
10
20
60
150
300
1000
+
Amery Ice Shelf
Mason Peaks
Progress Station
Ranvik Glacier
American Highland
Zhaojun Di
King Leopold and Queen Astrid Coast
Korotkevicha Plateau
Wilhelm II Land
Sovetskaya
90⁰E
SPRI-54/59
SPRI-60
C25SAE2
C25SAE1
Ridge B
SPRI-47
Vostok
Komsomolskoe
R15Ea_4
0 100 200 300 400 km

(b)

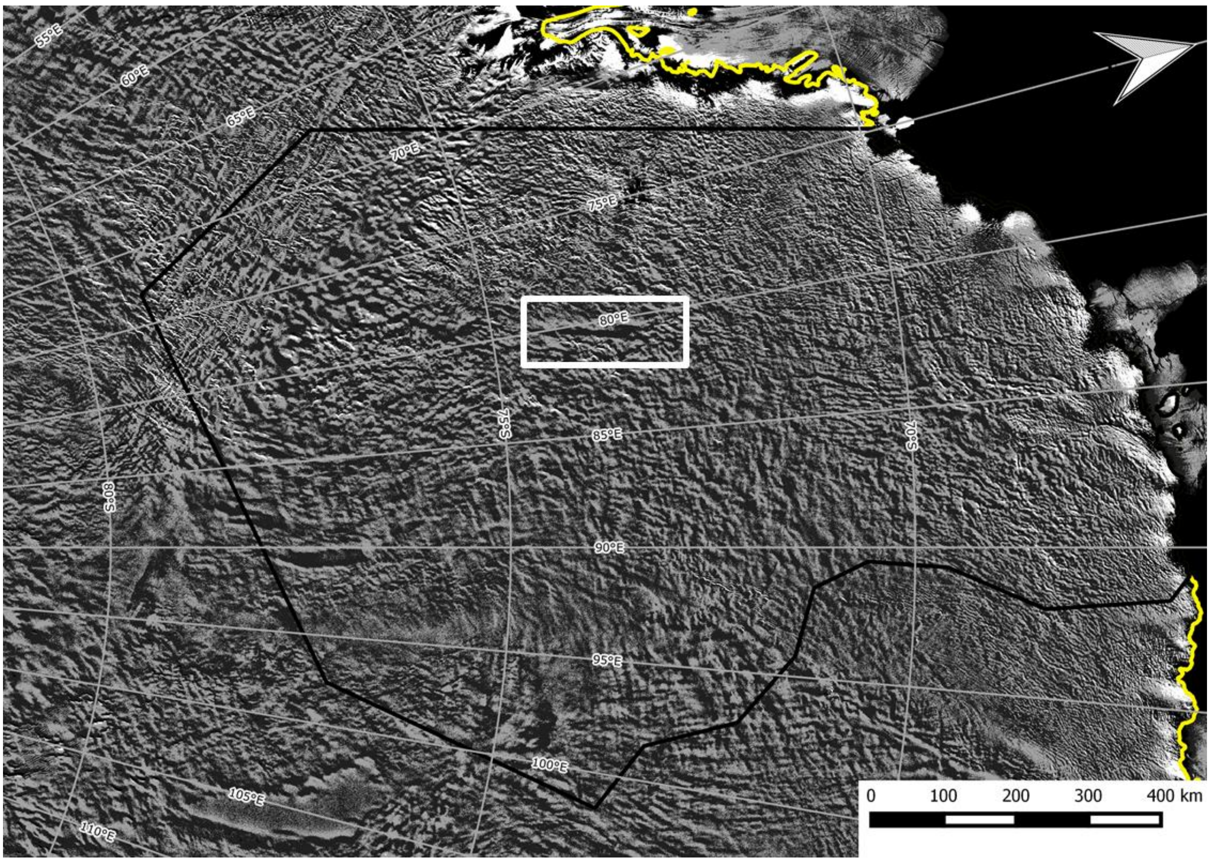
55°E
60°E
65°E
70°E
75°E
80°E
85°E
90°E
95°E
100°E
105°E
110°E
75°S
70°S
80°S
0 100 200 300 400 km

(c)

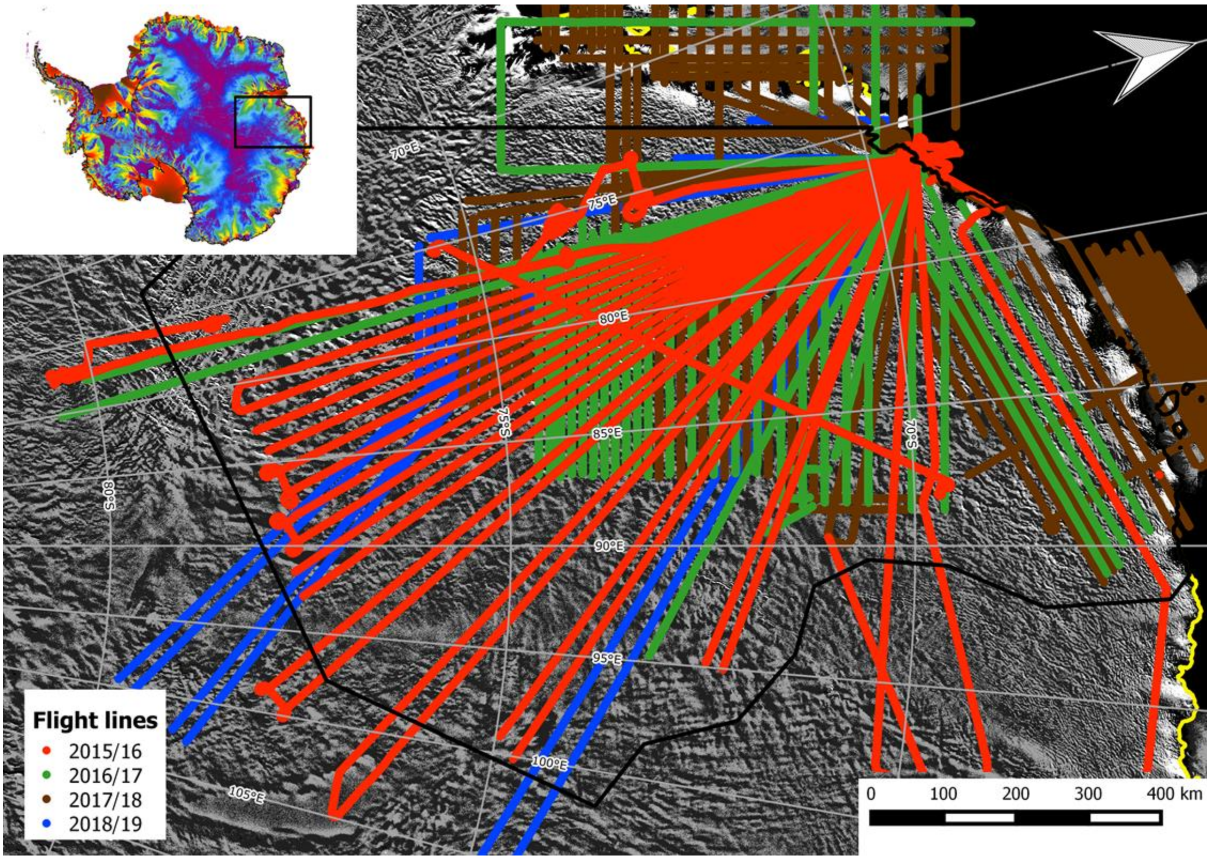

Figure 1. Map of (a) ice flow velocity version 2 (Rignot et al., 2017b); (b) MODIS Mosaic of Antarctica 2008–2009 satellite image (Haran et al., 2014). The black line denotes the grid boundary for ICECAP2 bed elevation model White box indicates a location of a previously discovered smooth-surface elongated and extensive feature interpreted as a potential subglacial lake (Jamieson et al., 2016); and (c) the Aerogeophysical flight lines surveyed by PRIC in four seasons which are 2015/16 (orange), 2016/17 (green), 2017/18 (red) and 2018/19 (blue) across the PEL sector; the inset denotes location of the study region in East Antarctica. Figures 1b and 1c are overlain by MODIS Mosaic of Antarctica 2008–2009 (Haran et al., 2014). The Differential Interferometry Synthetic Aperture Radar (DInSAR) grounding line (yellow line) are also shown (Rignot et al., 2017a).

(a)

(b)

(c)

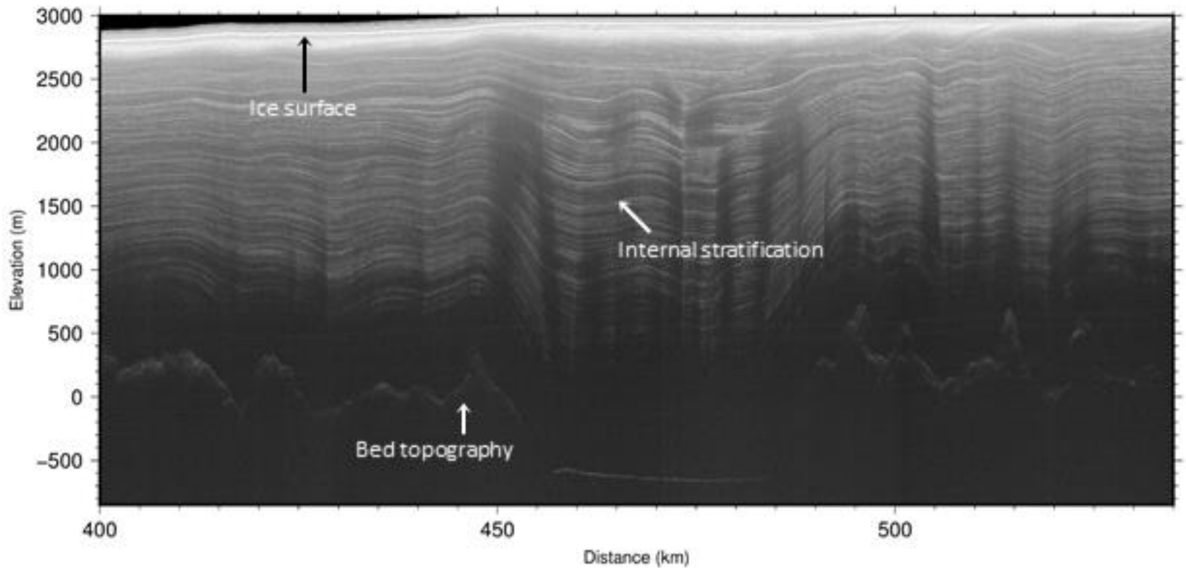

Figure 2. (a) Snow Eagle 601 airplane operated by the Polar Research Institute of China for the Chinese National Antarctic Research Expedition (CHINARE) program; (b) The interior image of the airplane showing the airborne radio-echo sounder equipment; and (c) Two-dimensional radio-echo sounding radargram collected in 2017/18 revealing the quality of internal layers, bed topography and subglacial lake water.

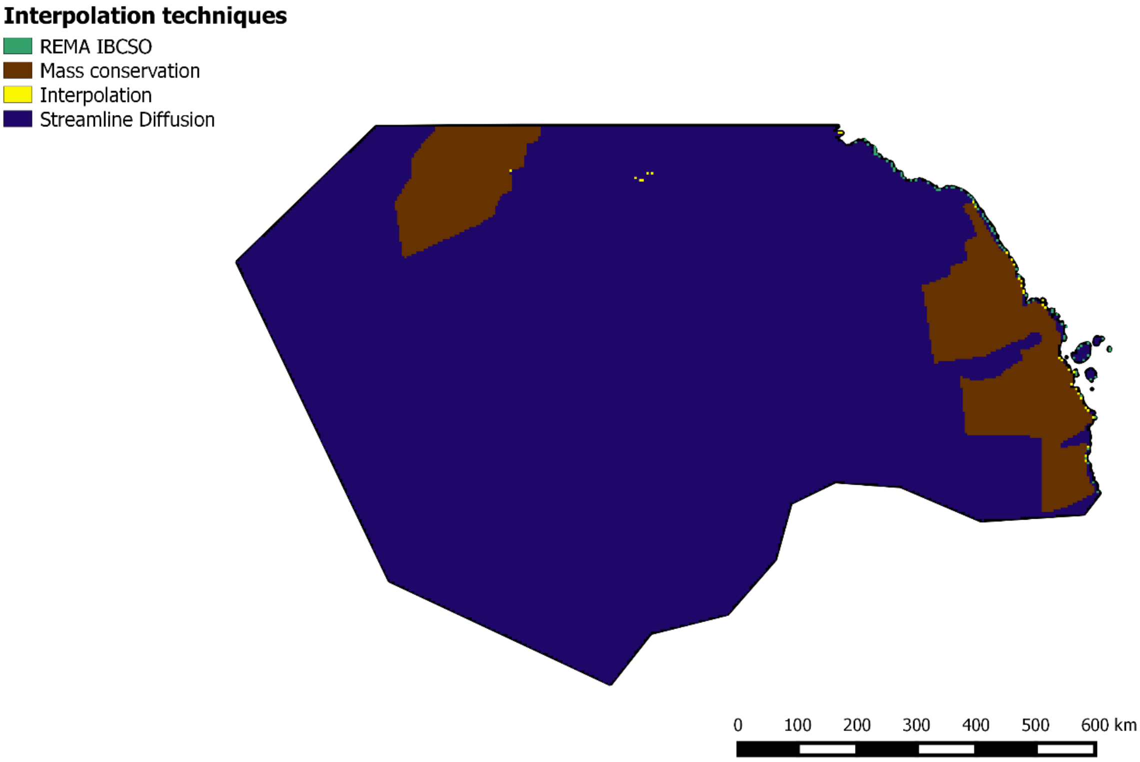

Figure 3. Map shows interpolation techniques used to infer ice thickness DEM across PEL, reference Elevation Model of Antarctica, International Bathymetric Chart of the Southern Ocean (REMA IBCSO, green), mass conservation (brown), interpolation (yellow) and streamline diffusion (blue).

(a)

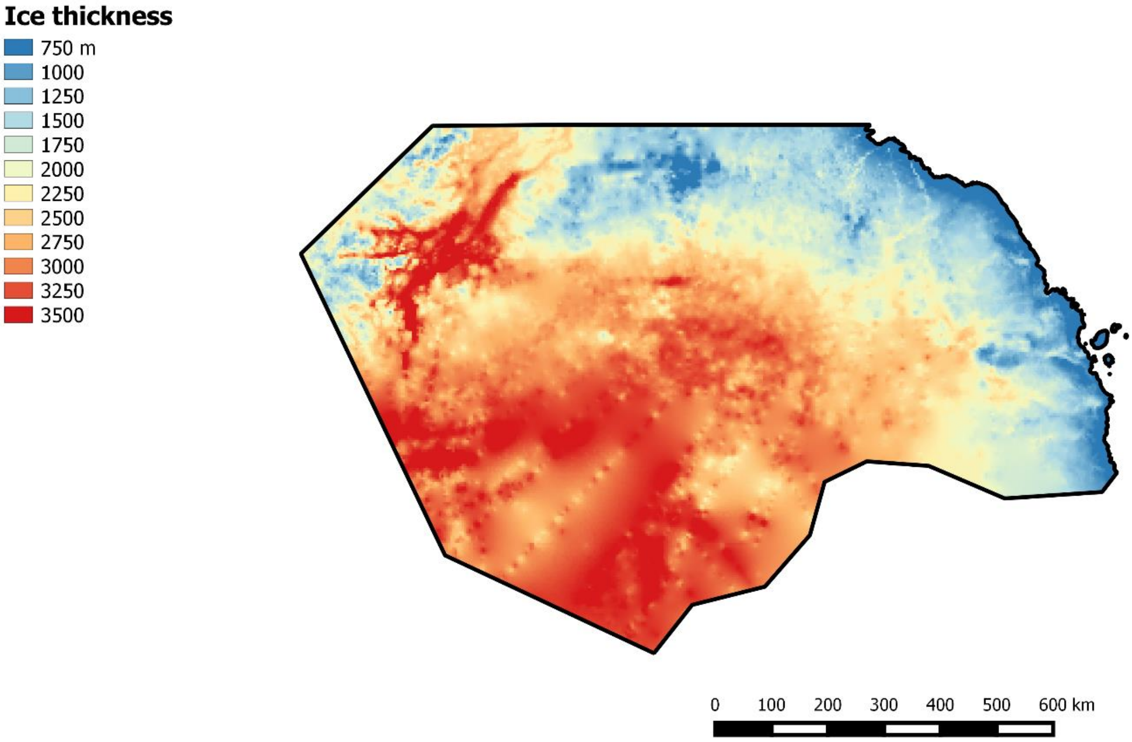
Ice thickness
750 m
1000
1250
1500
1750
2000
2250
2500
2750
3000
3250
3500
0 100 200 300 400 500 600 km

(b)

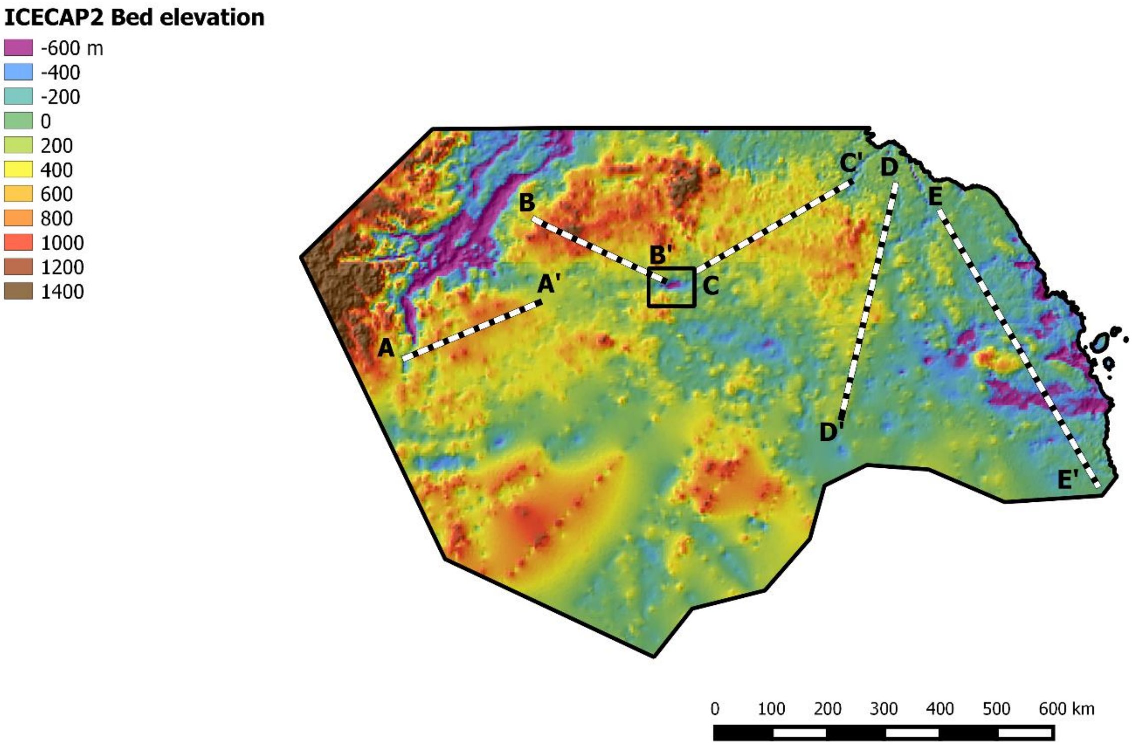
ICECAP2 Bed elevation
-600 m
-400
-200
0
200
400
600
800
1000
1200
1400
A
A'
B
B'
C
C'
D
D'
E
E'
0 100 200 300 400 500 600 km

(c)

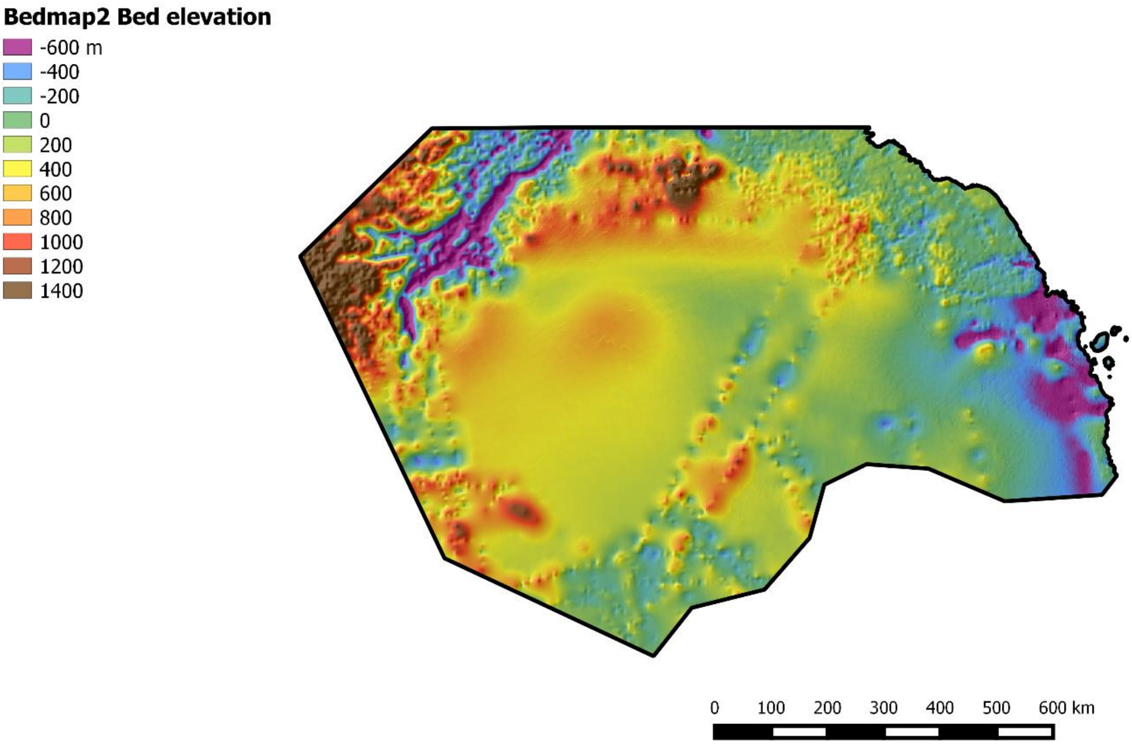
Bedmap2 Bed elevation
-600 m
-400
-200
0
200
400
600
800
1000
1200
1400
0 100 200 300 400 500 600 km

(d)

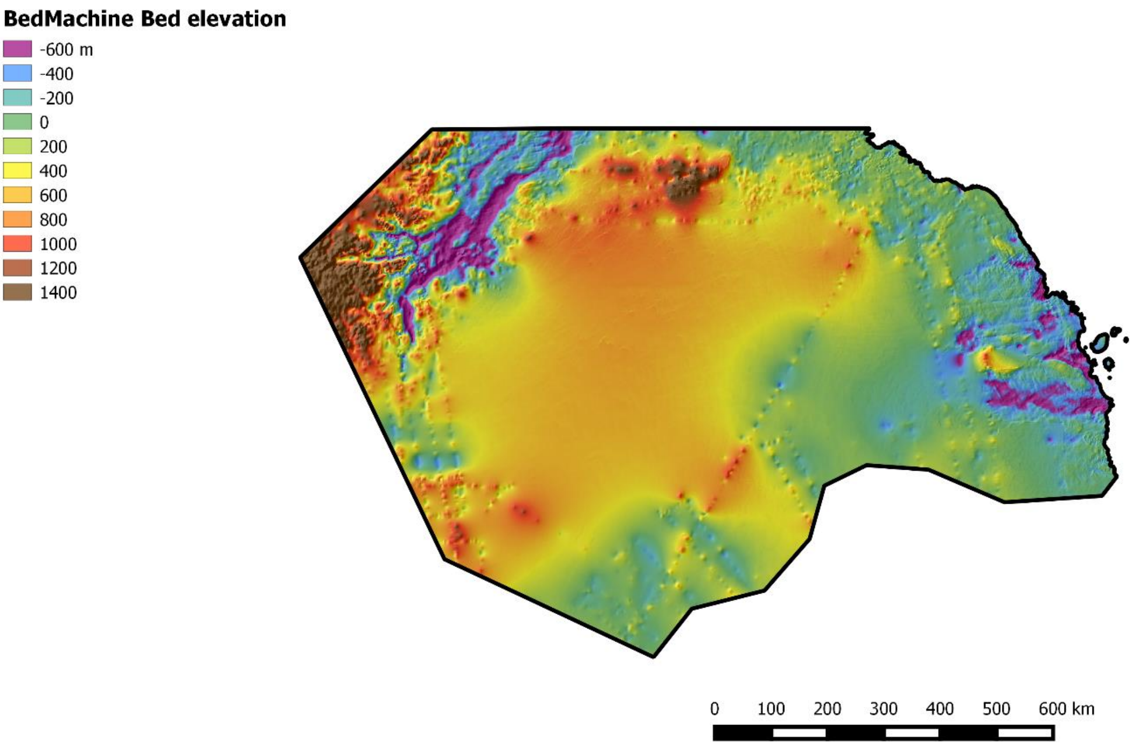
BedMachine Bed elevation
-600 m
-400
-200
0
200
400
600
800
1000
1200
1400
0 100 200 300 400 500 600 km

(e)

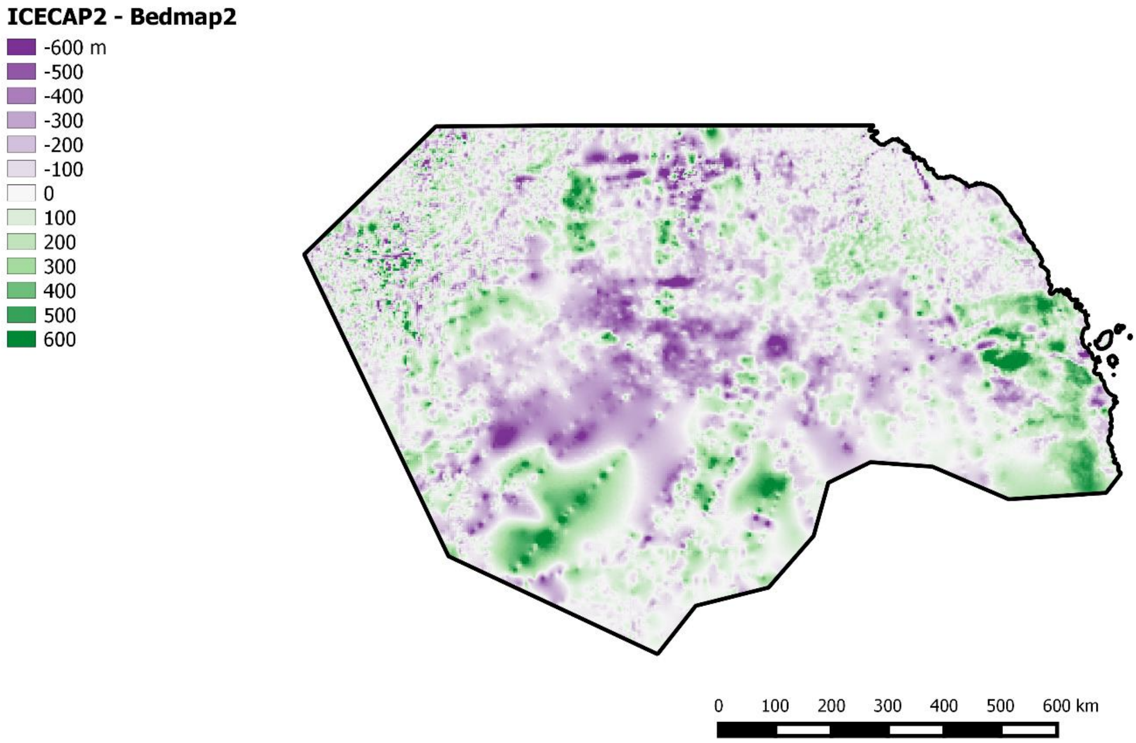
ICECAP2 - Bedmap2
-600 m
-500
-400
-300
-200
-100
0
100
200
300
400
500
600
0
100
200
300
400
500
600 km

(f)

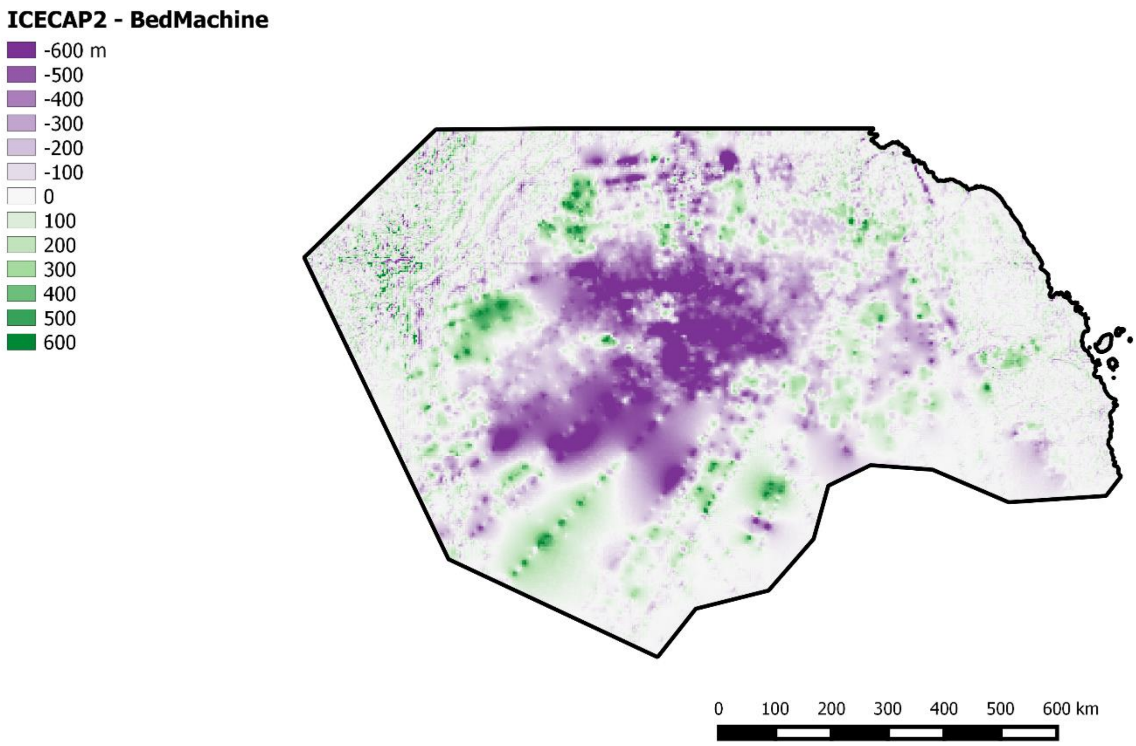
ICECAP2 - BedMachine
-600 m
-500
-400
-300
-200
-100
0
100
200
300
400
500
600
0
100
200
300
400
500
600 km

Figure 4. Bed elevation maps for Princess Elizabeth Land. (a) ICECAP2 ice thickness DEM derived using mass conservation; (b) ICECAP2 bed DEM for the PEL sector. Profiles A–A’, B–B’, C–C’, D–D’ and E–E’ are overlain in (b). The black box indicates a location of a previously discovered smooth-surface elongated and extensive feature interpreted as a potential subglacial lake (Jamieson et al., 2016). (c) Bedmap2 bed elevation model. (d) BedMachine bed elevation. (e) Difference map between the ICECAP2 and Bedmap2 DEMs; (f) Difference map between the ICECAP2 and BedMachine DEMs.

(a)

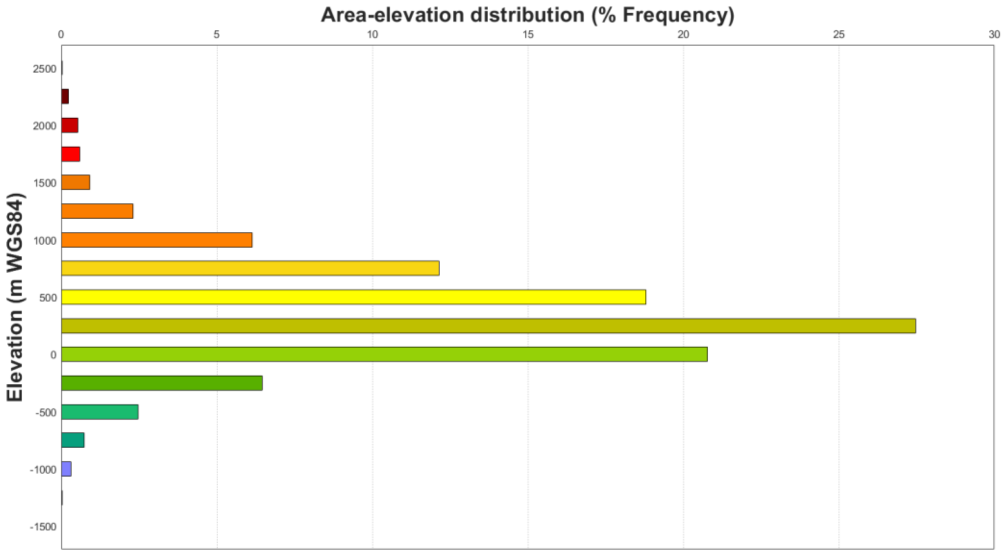

(b)

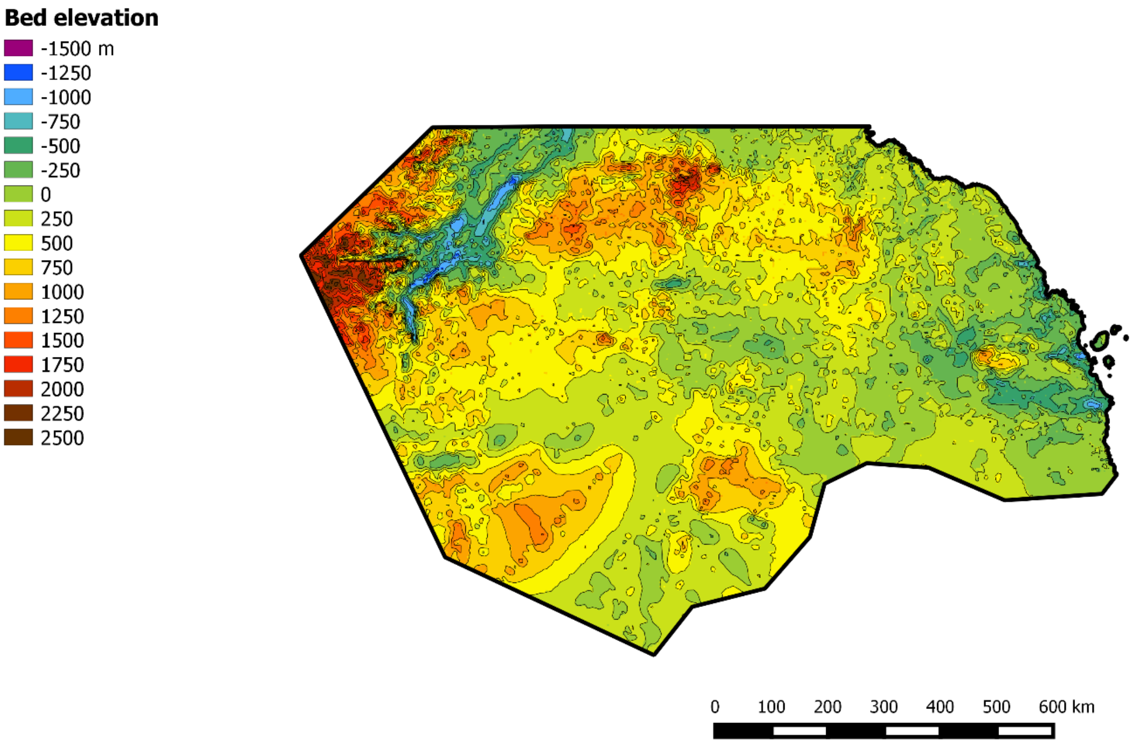

Figure 5. (a) Hypsometry (area-elevation distribution) derived from the ICECAP2 bed elevation model; and (b) Bed elevation model determined for the PEL sector, East Antarctica. The graph and map have the same elevation-related colour scheme.

(a)

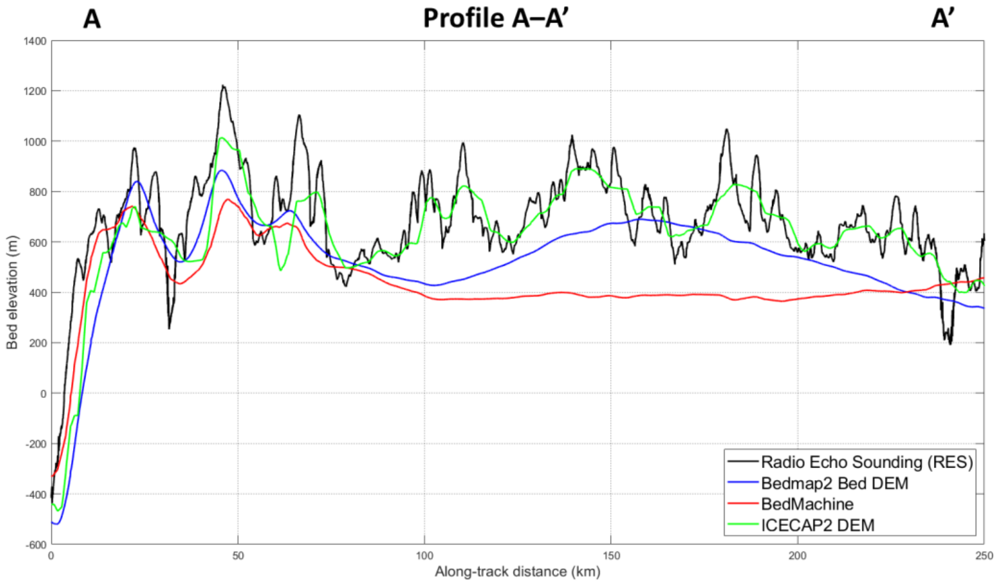
A
Profile A–A′
A′
Bed elevation (m)
Along-track distance (km)
Radio Echo Sounding (RES)
Bedmap2 Bed DEM
BedMachine
ICECAP2 DEM

(b)

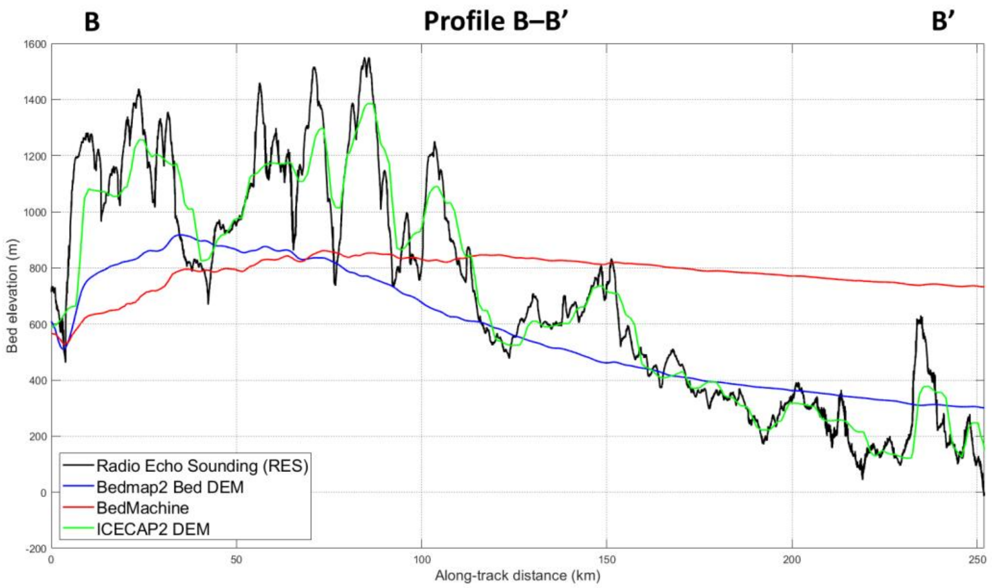
B
Profile B–B′
B′
Bed elevation (m)
Along-track distance (km)
Radio Echo Sounding (RES)
Bedmap2 Bed DEM
BedMachine
ICECAP2 DEM

(c)

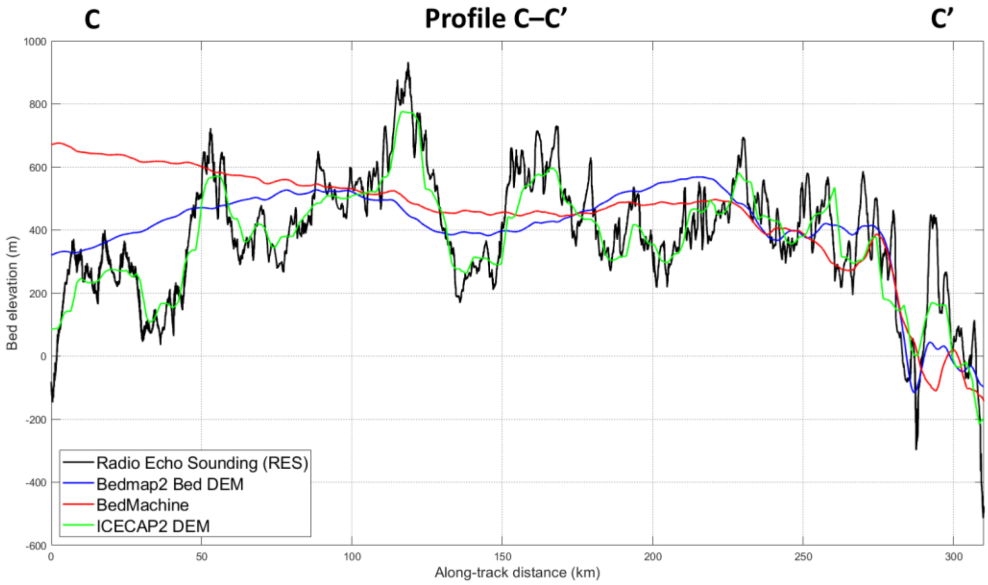

C
Profile C–C′
C′
Bed elevation (m)
Along-track distance (km)
Radio Echo Sounding (RES)
Bedmap2 Bed DEM
BedMachine
ICECAP2 DEM

(d)

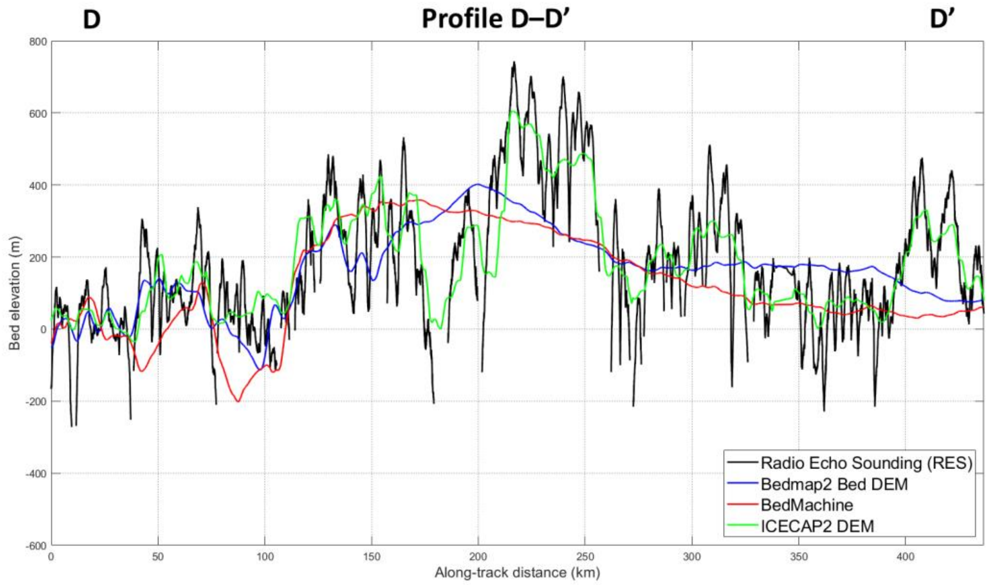

D
Profile D–D′
D′
Bed elevation (m)
Along-track distance (km)
Radio Echo Sounding (RES)
Bedmap2 Bed DEM
BedMachine
ICECAP2 DEM

362 (e)

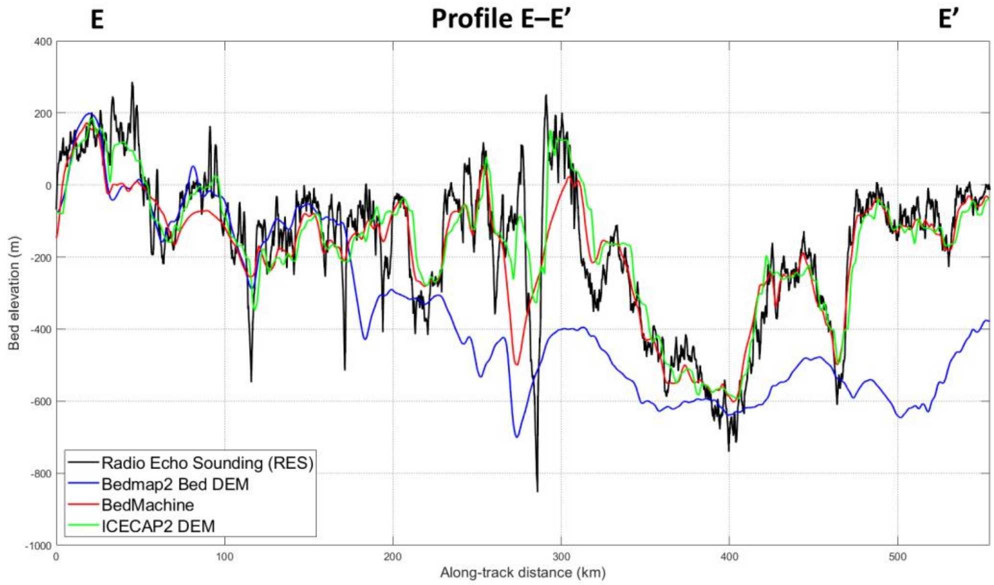

363

364 **Figure 6.** Bed elevations for RES transects (black), Bedmap2 (blue), BedMachine (red) and ICECAP 2 (green) for (a) Profile A–A', (b) Profile B–B', (c) Profile C–C', (d) Profile D–D' and (e) Profile E–E'.

366

367

REFERENCES

Bamber, J., Gomez-Dans, J., and Griggs, J.: A new 1 km digital elevation model of the Antarctic derived from combined satellite radar and laser data–Part 1: Data and methods, The Cryosphere, 3, 101-111, 2009.

Bingham, R. G. and Siegert, M. J.: Radar-derived bed roughness characterization of Institute and Möller ice streams, West Antarctica, and comparison with Siple Coast ice streams, Geophysical Research Letters, 34, L21504, 2007.

Blankenship, D. D., S. D. Kempf, D. A. Young, T. G. Richter, D. M. Schroeder, G. Ng, J. S. Greenbaum, T. van Ommen, R. C. Warner, J. L. Roberts, N. W. Young, E. Lemeur, and M. J. Siegert.: IceBridge HiCARS 2 L2 geolocated ice thickness, version 1. Boulder, Colorado, USA. NASA National Snow and Data Center Distributed Active Archive Center. https://doi.org/10.5067/9EBR2T0VXUDG, 2017.

Blankenship, D. D., S. D. Kempf, D. A. Young, T. G. Richter, D. M. Schroeder, J. S. Greenbaum, J. W. Holt, T. van Ommen, R. C. Warner, J. L. Roberts, N. W. Young, E. Lemeur, and M. J. Siegert.: IceBridge HiCARS 1 L2 geolocated ice thickness, Version 1. Boulder, Colorado, USA. NASA National Snow and Ice Data Center Distributed Active Archive Center. https://doi.org/10.5067/F5FGUT9F5089, 2016.

Cui, X., Greenbaum, J. S., Beem, L. H., Guo, J., Ng, G., Li, L., Blankenship, D., and Sun, B.: The First Fixed-wing Aircraft for Chinese Antarctic Expeditions: Airframe, modifications, Scientific Instrumentation and Applications, Journal of Environmental and Engineering Geophysics, 23, 1-13, 2018.

Cui, X., Jeofry, H., Greenbaum, J.S., Ross, N., Morlighem, M., Roberts, J.L., Blankenship, D.D., Bo, S., Siegert, M.J.: ICECAP-2 consortium bed elevation model for Princess Elizabeth Land, East Antarctica [Data set]. Zenodo. http://doi.org/10.5281/zenodo.4023343, 2020.

Dean, K., Naylor, S., and Siegert, M. Data in Antarctic Science and Politics. Social Studies of Science, 38/4, 571–604, 2008.

Diez, A., Matsuoka, K., Jordan, T. A., Kohler, J., Ferraccioli, F., Corr, H. F., Olesen, A.V. Forsberg, R., and Casal, T.G.: Patchy lakes and topographic origin for fast flow in the Recovery Glacier system, East Antarctica. Journal of Geophysical Research: Earth Surface, 124, 287–304. https://doi.org/10.1029/2018JF004799, 2019.

Dongchen, E., Zhou, C., and Liao, M.: Application of SAR interferometry on DEM generation of the Grove Mountains, Photogrammetric Engineering & Remote Sensing, 70, 1145-1149, 2004.

Dowdeswell, J. A. and Evans, S.: Investigations of the form and flow of ice sheets and glaciers using radio-echo sounding, Reports on Progress in Physics, 67, 1821, 2004.

Drewry, D. and Meldrum, D.: Antarctic airborne radio echo sounding, 1977–78, Polar Record, 19, 267-273, 1978.

Drewry, D., Meldrum, D., and Jankowski, E.: Radio echo and magnetic sounding of the Antarctic ice sheet, 1978–79, Polar Record, 20, 43-51, 1980.

Drewry, D. J.: Antarctica, Glaciological and Geophysical Folio, Scott Polar Research Institute, University of Cambridge, Cambridge, UK, 1983.

Fretwell, P., Pritchard, H. D., Vaughan, D. G., Bamber, J. L., Barrand, N. E., Bell, R., Bianchi, C., Bingham, R. G., Blankenship, D. D., Casassa, G., Catania, G., Callens, D., Conway, H., Cook, A. J., Corr, H. F. J., Damaske, D., Damm, V., Ferraccioli, F., Forsberg, R., Fujita, S., Gim, Y., Gogineni, P., Griggs, J. A., Hindmarsh, R. C. A., Holmlund, P., Holt, J. W., Jacobel, R. W., Jenkins, A., Jokat, W., Jordan, T., King, E. C., Kohler, J., Krabill, W., Riger-Kusk, M., Langley, K. A., Leitchenkov, G., Leuschen, C., Luyendyk, B. P., Matsuoka, K., Mouginot, J., Nitsche, F. O., Nogi, Y., Nost, O. A., Popov, S. V., Rignot, E., Rippin, D. M., Rivera, A., Roberts, J., Ross, N., Siegert, M. J., Smith, A. M., Steinhage, D., Studinger, M., Sun, B., Tinto, B. K., Welch, B. C., Wilson, D., Young, D. A., Xiangbin, C., and Zirizzotti, A.: Bedmap2: improved ice bed, surface and thickness datasets for Antarctica, The Cryosphere, 7, 375-393, 2013.

Greenbaum, J. S., Blankenship, D. D., Young, D. A., Richter, T. G., Roberts, J. L., Aitken, A. R. A., Legresy, B., Schroeder, D. M., Warner, R. C., van Ommen, T. D., and Siegert, M. J.: Ocean access to a cavity beneath Totten Glacier in East Antarctica, Nature Geoscience, 8, 294-298, 2015.

Haran, T., Bohlander, J., Scambos, T., Painter, T., and Fahnestock, M.: MODIS Mosaic of Antarctica 2008–2009 (MOA 2009) Image Map, National Snow and Ice Data Center, Boulder, Colorado, USA, 2014.

Helm, V., Humbert, A., and Miller, H.: Elevation and elevation change of Greenland and Antarctica derived from CryoSat-2, The Cryosphere, 8, 1539-1559, 2014.

Howat, I. M., Porter, C., Smith, B. E., Noh, M.-J., and Morin, P.: The Reference Elevation Model of Antarctica, The Cryosphere, 13, 665-674, 2019.

Jamieson, S. S., Ross, N., Greenbaum, J. S., Young, D. A., Aitken, A. R., Roberts, J. L., Blankenship, D. D., Bo, S., and Siegert, M. J.: An extensive subglacial lake and canyon system in Princess Elizabeth Land, East Antarctica, Geology, 44, 87-90, 2016.

Jankowski, E. J. and Drewry, D.: The structure of West Antarctica from geophysical studies, Nature, 291, 17-21, 1981.

Jordan, T. A., Martin, C., Ferraccioli, F., Matsuoka, K., Corr, H., Forsberg, R., Olesen, A., & Siegert, M. J.: Anomalously high geothermal flux near the South Pole. Scientific Reports, 8 (1). https://doi.org/10.1038/s41598-018-35182-0, 2018.

Lythe, M. B., Vaughan, D. G., and Consortium, T. B.: BEDMAP: A new ice thickness and subglacial topographic model of Antarctica, Journal of Geophysical Research: Solid Earth, 106, 11335-11351, 2001.

Morlighem, M., Rignot, E., Binder, T., Blankenship, D., Drews, R., Eagles, G., Eisen, O., Ferraccioli, F., Forsberg, R., Fretwell, P., Goel, V., Greenbaum, J. S., Gudmundsson, H., Guo, J., Helm, V., Hofstede, C., Howat, I., Humbert, A., Jokat, W., Karlsson, N. B., Lee, W. S., Matsuoka, K., Millan, R., Mouginot, J., Paden, J., Pattyn, F., Roberts, J., Rosier, S., Ruppel, A., Seroussi, H., Smith, E. C., Steinhage, D., Sun, B., Broeke, M. R. v. d., Ommen, T. D. v., Wessem, M. v., and Young, D. A.: Deep glacial troughs and stabilizing ridges unveiled beneath the margins of the Antarctic ice sheet, Nature Geoscience, 13, 132-137, 2020.

Naylor, S., Dean, K., and Siegert, M.J. The IGY and the ice sheet: surveying Antarctica. Journal of Historical Geography, 34, 574-595, 2008.

Peters, M. E., Blankenship, D. D., Carter, S. P., Kempf, S. D., Young, D. A., and Holt, J. W.: Along-Track Focusing of Airborne Radar Sounding Data From West Antarctica for Improving Basal Reflection Analysis and Layer Detection, IEEE Transactions on Geoscience and Remote Sensing, 45, 2725-2736, 2007.

Popov, S.: Fifty-five years of Russian radio-echo sounding investigations in Antarctica, Annals of Glaciology, doi: 10.1017/aog.2020.4, 2020. 1-11, 2020.

Popov, S. and Kiselev, A.: Russian airborne geophysical investigations of Mac. Robertson, Princess Elizabeth and Wilhelm II Lands, East Antarctica, Earth's Cryosphere, 22, 1-12, 2018.

Rignot, E., Mouginot, J., and Scheuchl, B.: Antarctic grounding line mapping from differential satellite radar interferometry, Geophysical Research Letters, 38, L10504, 2011.

Rignot, E., Mouginot, J., and Scheuchl, B.: MEaSUREs Antarctic Grounding Line from Differential Satellite Radar Interferometry, Version 2, National Snow and Ice Data Center, Boulder, Colorado, USA, 2017a.

Rignot, E., Mouginot, J., and Scheuchl, B.: MEaSUREs InSAR-Based Antarctica Ice Velocity Map, Version 2, National Snow and Ice Data Center, Boulder, Colorado, USA, 2017b.

Robin, G. d. Q., Drewry, D., and Meldrum, D.: International studies of ice sheet and bedrock, Philosophical Transactions of the Royal Society of London. B, Biological Sciences, 279, 185-196, 1977.

Snyder, J. P.: Map projections-A Working Manual, United States Government Printing Office, Washington, D.C., USA, 1987.

Turchetti, S., Dean, K., Naylor, S., and Siegert, M. Accidents and Opportunities: A History of the Radio Echo Sounding (RES) of Antarctica, 1958-1979. British Journal of the History of Science, 41, 417-444, 2008.

Young, D. A., Wright, A. P., Roberts, J. L., Warner, R. C., Young, N. W., Greenbaum, J. S., Schroeder, D. M., Holt, J. W., Sugden, D. E., Blankenship, D. D., van Ommen, T. D., and Siegert, M. J.: A dynamic early East Antarctic Ice Sheet suggested by ice-covered fjord landscapes, Nature, 474, 72-75, 2011.